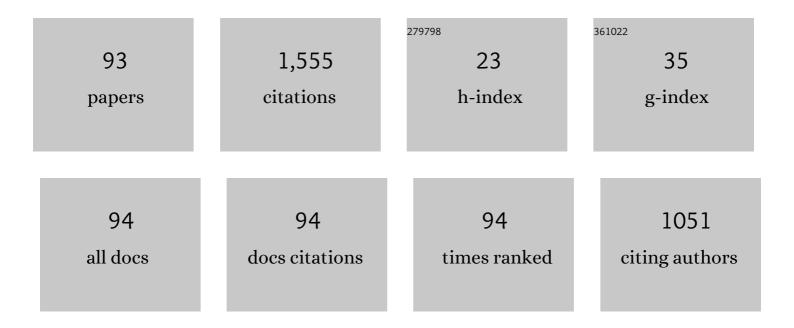
Werner Ecker

List of Publications by Year in descending order

Source: https://exaly.com/author-pdf/3171352/publications.pdf Version: 2024-02-01



#	Article	lF	CITATIONS
1	X-ray nanodiffraction reveals strain and microstructure evolution in nanocrystalline thin films. Scripta Materialia, 2012, 67, 748-751.	5.2	103
2	X-ray analysis of residual stress gradients in TiN coatings by a Laplace space approach and cross-sectional nanodiffraction: a critical comparison. Journal of Applied Crystallography, 2013, 46, 1378-1385.	4.5	78
3	Finite element study of the influence of hard coatings on hard metal tool loading during milling. Surface and Coatings Technology, 2016, 304, 134-141.	4.8	57
4	X-ray nanodiffraction reveals stress distribution across an indented multilayered CrN–Cr thin film. Acta Materialia, 2015, 85, 24-31.	7.9	53
5	In-situ Observation of Cross-Sectional Microstructural Changes and Stress Distributions in Fracturing TiN Thin Film during Nanoindentation. Scientific Reports, 2016, 6, 22670.	3.3	52
6	Critical assessment of the determination of residual stress profiles in thin films by means of the ion beam layer removal method. Thin Solid Films, 2014, 564, 321-330.	1.8	51
7	Experimental and numerical investigations of the γ″ and γ′ precipitation kinetics in Alloy 718. Materials Science & Engineering A: Structural Materials: Properties, Microstructure and Processing, 2018, 723, 314-323.	5.6	50
8	Microstructural based hydrogen diffusion and trapping models applied to Fe–C X alloys. Journal of Alloys and Compounds, 2020, 826, 154057.	5.5	50
9	Model-based interpretation of thermal desorption spectra of Fe-C-Ti alloys. Journal of Alloys and Compounds, 2019, 789, 647-657.	5.5	47
10	The influence of alloying on Zn liquid metal embrittlement in steels. Acta Materialia, 2020, 195, 750-760.	7.9	45
11	Hydrogen Trapping in bcc Iron. Materials, 2020, 13, 2288.	2.9	42
12	Lateral gradients of phases, residual stress and hardness in a laser heated Ti0.52Al0.48N coating on hard metal. Surface and Coatings Technology, 2012, 206, 4502-4510.	4.8	37
13	Hydrogen-enhanced decohesion mechanism of the special <mml:math xmlns:mml="http://www.w3.org/1998/Math/MathML" altimg="si55.svg"><mml:mrow><mml:mi mathvariant="normal">Ĵ£</mml:mi </mml:mrow>5(0 1 2)[1 0 0] grain boundary in Ni with Mo and C solutes. Computational Materials Science. 2019. 167. 100-110.</mml:math 	3.0	37
14	Grain boundary segregation in Ni-base alloys: A combined atom probe tomography and first principles study. Acta Materialia, 2021, 221, 117354.	7.9	37
15	FE temperature- and residual stress prediction in milling inserts and correlation with experimentally observed damage mechanisms. Journal of Materials Processing Technology, 2018, 256, 98-108.	6.3	36
16	A microstructural based creep model applied to alloy 718. International Journal of Plasticity, 2018, 105, 62-73.	8.8	36
17	Kinetics of interaction of impurity interstitials with dislocations revisited. Progress in Materials Science, 2019, 101, 172-206.	32.8	34
18	Thermodynamic and mechanical stability of Ni3X-type intermetallic compounds. Intermetallics, 2019, 114, 106604.	3.9	33

WERNER ECKER

#	Article	IF	CITATIONS
19	Thermal crack formation in TiCN/α-Al2O3 bilayer coatings grown by thermal CVD on WC-Co substrates with varied Co content. Surface and Coatings Technology, 2020, 392, 125687.	4.8	32
20	Hydrogen-enhanced intergranular failure of sulfur-doped nickel grain boundary: In situ electrochemical micro-cantilever bending vs.ÂDFT. Materials Science & Engineering A: Structural Materials: Properties, Microstructure and Processing, 2020, 794, 139967.	5.6	27
21	Cyclic heat-up and damage-relevant substrate plastification of single- and bilayer coated milling inserts evaluated numerically. Surface and Coatings Technology, 2019, 360, 39-49.	4.8	26
22	Effect of alloying elements on hydrogen enhanced decohesion in bcc iron. Computational Materials Science, 2021, 188, 110215.	3.0	25
23	Residual stress and microstructure depth gradients in nitrided iron-based alloys revealed by dynamical cross-sectional transmission X-ray microdiffraction. Acta Materialia, 2015, 87, 100-110.	7.9	24
24	Stress relaxation through thermal crack formation in CVD TiCN coatings grown on WC-Co with different Co contents. International Journal of Refractory Metals and Hard Materials, 2020, 86, 105102.	3.8	24
25	On the local evaluation of the hydrogen susceptibility of cold-formed and heat treated advanced high strength steel (AHSS) sheets. Materials Science & Engineering A: Structural Materials: Properties, Microstructure and Processing, 2021, 800, 140276.	5.6	24
26	Effect of shot peening on residual stresses and crack closure in CVD coated hard metal cutting inserts. International Journal of Refractory Metals and Hard Materials, 2019, 82, 174-182.	3.8	23
27	Cycled hydrogen permeation through Armco iron – A joint experimental and modeling approach. Corrosion Science, 2020, 176, 109017.	6.6	23
28	Shot peening-induced plastic deformation of individual phases within a coated WC-Co hard metal composite material including stress-strain curves for WC as a function of temperature. Surface and Coatings Technology, 2019, 380, 125026.	4.8	18
29	Nanoscale evolution of stress concentrations and crack morphology in multilayered CrN coating during indentation: Experiment and simulation. Materials and Design, 2020, 188, 108478.	7.0	18
30	Local hydrogen accumulation after cold forming and heat treatment in punched advanced high strength steel sheets. Journal of Alloys and Compounds, 2021, 856, 158226.	5.5	18
31	Hydrogen segregation near a crack tip in nickel. Scripta Materialia, 2021, 194, 113697.	5.2	18
32	Tensile stresses in fine blanking tools and their relevance to tool fracture behavior. International Journal of Machine Tools and Manufacture, 2018, 126, 44-50.	13.4	17
33	Verification of the generalised chemical potential for stress-driven hydrogen diffusion in nickel. Philosophical Magazine Letters, 2020, 100, 513-523.	1.2	16
34	LESâ€VOF Simulation and POD Analysis of the Gasâ€Jet Wiping Process in Continuous Galvanizing Lines. Steel Research International, 2018, 89, 1700362.	1.8	15
35	Residual stress and microstructure evolution in steel tubes for different cooling conditions – Simulation and verification. Materials Science & Engineering A: Structural Materials: Properties, Microstructure and Processing, 2019, 747, 73-79.	5.6	14
36	An SEM compatible plasma cell for <i>in situ</i> studies of hydrogen-material interaction. Review of Scientific Instruments, 2020, 91, 043705.	1.3	13

WERNER ECKER

#	Article	lF	CITATIONS
37	Differences in evolution of temperature, plastic deformation and wear in milling tools when up-milling and down-milling Ti6Al4V. Journal of Manufacturing Processes, 2022, 77, 75-86.	5.9	12
38	Thermal fatigue behaviour of hot-work tool steels: heat check nucleation and growth. International Journal of Microstructure and Materials Properties, 2008, 3, 182.	0.1	11
39	Cross-sectional stress distribution in Al x Ga 1-x N heterostructure on Si(111) substrate characterized by ion beam layer removal method and precession electron diffraction. Materials and Design, 2016, 106, 476-481.	7.0	11
40	Strength ranking for interfaces between a TiN hard coating and microstructural constituents of high speed steel determined by micromechanical testing. Materials and Design, 2021, 204, 109690.	7.0	11
41	Addressing H-Material Interaction in Fast Diffusion Materials—A Feasibility Study on a Complex Phase Steel. Materials, 2020, 13, 4677.	2.9	10
42	Strain ratcheting limit stresses as a function of microstructure of WC-Co hardmetals under uniaxial cyclic loads under a stress ratio of RÂ=Ââ~'â^ž at elevated temperatures. International Journal of Refractory Metals and Hard Materials, 2022, 102, 105699.	3.8	10
43	Creep behaviour of WC-12Âwt% Co hardmetals with different WC grain sizes tested in uniaxial tensile and compression step-loading tests at 700°C and 800°C. International Journal of Refractory Metals and Hard Materials, 2021, 100, 105633.	3.8	10
44	The effect of solute atoms on the bulk and grain boundary cohesion in Ni: Implications for hydrogen embrittlement. Materialia, 2022, 21, 101293.	2.7	10
45	Verification of a continuum mechanical explanation of plasticity-induced crack closure under plain strain conditions by means of finite element analysis. Engineering Fracture Mechanics, 2012, 96, 762-765.	4.3	9
46	A physical reason for asymmetric creep deformation behaviour of WC-Co hardmetal under tension and compression loading at 700°C and 800°C. International Journal of Refractory Metals and Hard Materials, 2021, 97, 105526.	3.8	9
47	Size Effects in Residual Stress Formation during Quenching of Cylinders Made of Hot-Work Tool Steel. Advances in Materials Science and Engineering, 2015, 2015, 1-7.	1.8	8
48	Error Analysis for Finite Element Simulation of Orthogonal Cutting and its Validation Via Quick Stop Experiments. Machining Science and Technology, 2015, 19, 460-478.	2.5	8
49	Analysis of shape, orientation and interface properties of Mo <mml:math xmlns:mml="http://www.w3.org/1998/Math/MathML" altimg="si15.svg"><mml:msub><mml:mrow /><mml:mn>2</mml:mn></mml:mrow </mml:msub>C precipitates in Fe using ab-initio and finite element method calculations. Acta Materialia. 2021. 204. 116478.</mml:math 	7.9	8
50	Experimentelle und numerische Untersuchung des induktiven Anlassens eines Vergütungsstahles*. HTM - Journal of Heat Treatment and Materials, 2017, 72, 199-204.	0.2	8
51	Hydrogen assisted intergranular cracking of alloy 725: The effect of boron and copper alloying. Corrosion Science, 2022, 203, 110331.	6.6	8
52	Using Finite Element Simulation to Optimize the Heat Treatment of Tire Protection Chains. Journal of Materials Engineering and Performance, 2014, 23, 1288-1295.	2.5	7
53	Numerical calibration of a yield limit function for rock materials by means of the Brazilian test and the uniaxial compression test. International Journal of Rock Mechanics and Minings Sciences, 2015, 74, 24-29.	5.8	7
54	Thermo-chemical Fluid Flow Simulation in Hot-Dip Galvanizing: The Evaluation of Dross Build-Up Formation. Metallurgical and Materials Transactions B: Process Metallurgy and Materials Processing Science, 2019, 50, 834-845.	2.1	7

WERNER ECKER

#	Article	IF	CITATIONS
55	Correlative cross-sectional characterization of nitrided, carburized and shot-peened steels: synchrotron micro-X-ray diffraction analysis of stress, microstructure and phase gradients. Journal of Materials Research and Technology, 2021, 11, 1396-1410.	5.8	7
56	Validated Multi-Physical Finite Element Modelling of the Spot Welding Process of the Advanced High Strength Steel DP1200HD. Materials, 2021, 14, 5411.	2.9	7
57	Damage indicators for early fatigue damage assessment in WC-Co hardmetals under uniaxial cyclic loads at a stress ratio of RÂ=Ââ °1 at elevated temperatures. International Journal of Refractory Metals and Hard Materials, 2022, 103, 105749.	3.8	7
58	Cu-SiO2 hybrid bonding simulation including surface roughness and viscoplastic material modeling: A critical comparison of 2D and 3D modeling approach. Microelectronics Reliability, 2018, 86, 1-9.	1.7	6
59	Dark-field X-ray microscopy reveals mosaicity and strain gradients across sub-surface TiC and TiN particles in steel matrix composites. Scripta Materialia, 2020, 187, 402-406.	5.2	6
60	Micromechanics-based damage model for liquid-assisted healing. International Journal of Damage Mechanics, 2021, 30, 123-144.	4.2	6
61	Liquid Metal Embrittlement of Advanced High Strength Steel: Experiments and Damage Modeling. Materials, 2021, 14, 5451.	2.9	6
62	Analysis of Sn-Bi Solders: X-ray Micro Computed Tomography Imaging and Microstructure Characterization in Relation to Properties and Liquid Phase Healing Potential. Materials, 2021, 14, 153.	2.9	6
63	Thermodynamic trapping and diffusion model for multiple species in systems with multiple sorts of traps. Acta Materialia, 2022, 233, 117940.	7.9	6
64	Resolving alternating stress gradients and dislocation densities across AlxGa1-xN multilayer structures on Si(111). Applied Physics Letters, 2017, 111, 162103.	3.3	5
65	Influence of localized cyclic substrate plastification on residual stress, load stress and cracking near the interface between hard coating and WC-Co hard metal substrate. International Journal of Refractory Metals and Hard Materials, 2019, 82, 113-120.	3.8	5
66	An atomistic view on Oxygen, antisites and vacancies in the <mml:math xmlns:mml="http://www.w3.org/1998/Math/MathML" altimg="si165.svg"><mml:mrow><mml:mi>l³</mml:mi></mml:mrow>-TiAl phase. Computational Materials Science, 2021, 197, 110655.</mml:math 	3.0	5
67	On the transition of failure control from material-intrinsic defects to defects forming during monotonically increasing and cyclic mechanical loading in WC-Co hard metal at elevated temperature. Acta Materialia, 2022, 235, 118087.	7.9	5
68	Numerical Simulation of Crack Growth in Polyethylene Composites by Means of the Cohesive Zone Model. Macromolecular Symposia, 2012, 311, 1-8.	0.7	4
69	Inverse Model for the Control of Induction Heat Treatments. Materials, 2019, 12, 2826.	2.9	4
70	Nanoscale stress distributions and microstructural changes at scratch track cross-sections of a deformed brittle-ductile CrN-Cr bilayer. Materials and Design, 2020, 195, 109023.	7.0	4
71	Elasto-Viscoplastic Material Model of a Directly-Cast Low-Carbon Steel at High Temperatures. Materials, 2020, 13, 2281.	2.9	4
72	Effect of solder joint size and composition on liquid-assisted healing. Microelectronics Reliability, 2021, 119, 114066.	1.7	4

Werner Ecker

#	Article	IF	CITATIONS
73	Model-Based Residual Stress Design in Multiphase Seamless Steel Tubes. Materials, 2020, 13, 439.	2.9	4
74	Simulation and experimental characterization of microporosity during solidification in Sn-Bi alloys. Materials and Design, 2021, 212, 110258.	7.0	4
75	Fatigue damage mechanisms and damage evolution near cyclically loaded edges. Bulletin of the Polish Academy of Sciences: Technical Sciences, 2010, 58, .	0.8	3
76	Finite element modeling of the residual stress evolution in forged and direct-aged alloy 718 turbine disks during manufacturing and its experimental validation. AlP Conference Proceedings, 2017, , .	0.4	3
77	Matching in-situ and ex-situ recorded stress gradients in an AlxGa1â^`xN Heterostructure: Complementary wafer curvature analyses in time and space. Scripta Materialia, 2018, 147, 50-54.	5.2	3
78	Numerical study on local effects of composition and geometry in self-healing solders. , 2019, , .		3
79	Hybrid modeling of induction hardening processes. Applications in Engineering Science, 2021, 5, 100030.	0.8	3
80	Combined experimental and numerical analysis of critical loading conditions for hard metal tool damage in titanium milling. Journal of Manufacturing Processes, 2022, 77, 125-137.	5.9	3
81	Calibration and Validation of an Elasto-Viscoplastic Material Model for a Hot Work Tool Steel Used in Pressure Casting Dies. Key Engineering Materials, 2007, 345-346, 685-688.	0.4	2
82	Interaction of Heat Checks in Aluminum Pressure Casting Dies and their Effect on Fatigue Life. Key Engineering Materials, 0, 488-489, 626-629.	0.4	2
83	Different Microstructures in the HAZ of Double Submerged Arc Welded Pipelines and How They Influence the Fatigue Crack Growth. , 2013, , .		2
84	Healing solders: A numerical investigation of damage-healing experiments. , 2020, , .		2
85	Calibration and Validation of an Elasto-Viscoplastic Material Model for a Hot Work Tool Steel Used in Pressure Casting Dies. Key Engineering Materials, 0, , 685-688.	0.4	2
86	Defect initiation and accumulation kinetics in hard-coated WC-Co hardmetal under multi-axial loads at elevated temperature in a novel ball-in-cone test setup. International Journal of Refractory Metals and Hard Materials, 2022, 104, 105785.	3.8	2
87	The cyclic elasto-viscoplastic behavior of a high-speed steel under forging conditions - experiments and simulations. Procedia Engineering, 2011, 10, 1991-1996.	1.2	1
88	Deep drawing of press hardening steels. Journal of Physics: Conference Series, 2018, 1063, 012038.	0.4	1
89	Selected Topics on Integrated Computational Material, Process, and Product Engineering. BHM-Zeitschrift Fuer Rohstoffe Geotechnik Metallurgie Werkstoffe Maschinen-Und Anlagentechnik, 2022, 167, 10-14.	1.0	1
90	Methodology for Advanced Tool Load Analysis. BHM-Zeitschrift Fuer Rohstoffe Geotechnik Metallurgie Werkstoffe Maschinen-Und Anlagentechnik, 2014, 159, 380-384.	1.0	0

Werner Ecker

#	Article	IF	CITATIONS
91	Experimental and computational approach to evaluate the effect of leveling on the change of tensile properites of heavy steel plates. AIP Conference Proceedings, 2017, , .	0.4	0
92	Lap shear test for solder materials: Local stress states and their effect on deformation and damage. Microelectronics Reliability, 2020, 109, 113655.	1.7	0
93	Modelling of Void Collapse with Molecular Dynamics in Pure Sn. Proceedings (mdpi), 2020, 56, .	0.2	0